Development of a Compact Lidar Sensor for Terrain Relative Navigation and Terrain Hazard Avoidance

Farzin Amzajerdian[*], Aram Gragossian [†], Paul F. Brewster[‡], Jacob M. Heppler[§], Frederick G. Wilson[**], Glenn D. Hines[††], Sean A. Laughter[‡‡], and Daniel K. Litton[§§]
NASA Langley Research Center, Hampton, VA 23681, USA

Alexander Bulyshev [***]
Coherent Applications Inc, Hampton, VA 23681, USA

A Lidar sensor utilizing linear-mode flash lidar technology and a novel Super-Resolution technique has been developed for providing Terrain Relative Navigation and Hazard Avoidance capabilities onboard landing vehicles. Processing algorithms for precision navigation and safe landing location identification take advantage of the uniform fixed pixels property of generated high resolution Digital Elevation Maps to achieve high reliability operation in near real-time. This paper describes the results of drone and helicopter flight tests of a breadboard system, explains the design and capabilities of a recently built compact prototype unit, and proposes a concepts of operation for future landing missions.

I. Introduction

Linear-mode flash lidar is recognized as one of the leading sensor technologies for enabling onboard Hazard Detection and Avoidance (HDA) required by many landing missions including manned and robotic missions to the Moon, Mars, and other planetary bodies [1,2]. The main advantage of flash lidar technology over more conventional scanning lidar is the ability to record full 3-D images with a single laser pulse, freezing the scene on every frame by removing all motion of the transmitter/receiver platform [3,4]. Unlike scanning imaging lidar systems that generate 3-D images by scanning the laser beam across the scene and measuring the time of arrival for each returned laser pulse, a flash lidar records a full 3-D image frame by illuminating the scene with a single laser pulse and imaging the scene onto one Focal Plane Array (FPA). Each pixel in the FPA takes independent measurements of the lidar pulse time of flight to the target. Therefore, the flash lidar does not require position and attitude angle data from external sensors and extensive computation resources and time for compensating vehicle motion during image acquisition. Another advantage is having uniformly distributed pixels with each image frame which simplifies the hazard detection algorithm and reduces the risk of false alarms [5].

But, flash lidars have limited resolution that may be insufficient for many applications. The number of pixels of linear-mode flash lidars is constrained by multiple factors including manufacturing limitations and required laser pulse energy and receiver aperture size for collecting enough returned photons for each pixel to generate a range image. Current commercially available linear-mode flash lidar focal plane array has 128 x 128 pixels which is grossly insufficient for mapping the designated landing area with the necessary Ground Sample Distance (GSD) for meeting the HDA requirements. Adjusting the Field-Of-View (FOV) of this flash lidar to cover a 100 m x 100 m area will give a GSD of 78 cm (100 m/128), which is much greater than the 15 cm GSD needed for reliably detecting 30 cm diameter hazards required by most landing missions. To overcome this shortcoming, past

[*] Principle Investigator, LaRC Remote Sensing Branch, Engineering Directorate.
[†] System Development Lead, LaRC Remote Sensing Branch, Engineering Directorate.
[‡] SW Lead, LaRC Flight Software Branch, Engineering Directorate.
[§] M.E. Lead, LaRC Mechanical Systems Branch, Engineering Directorate.
[**] E-O Lead, LaRC Remote Sensing Branch, Engineering Directorate.
[††] Chief Engineer, Engineering Directorate.
[‡‡] System Engineer, Engineering Integration Branch, Engineering Directorate.
[§§] Project Manager, Space Technology and Exploration Directorate.
[***] Algorithms Lead and System Analyst, LaRC Remote Sensing Branch, Engineering Directorate.

demonstration flight tests used a mechanical gimbal to scan the target area and stitch individual image frames with sufficiently small FOV and GSD [6]. But accommodation of a mechanical gimbal on landing vehicles is very challenging or even impractical. For this reason, we employ a novel Super-Resolution (SR) technique [7,8] to eliminate the mechanical gimbal.

In SR operation, the lidar FOV is enlarged to cover the whole area of interest and then a sequence of image frames of the same scene, taken from different positions and look angles, are blended to achieve the desired resolution. Our SR algorithm does not require position and attitude (pointing angle) data from an external sensor thus making the flash lidar a standalone instrument. In addition to eliminating the need for a scanning gimbal, the SR has several important advantages over stitching individual image frames. The SR technique lowers range measurement noise, recovers bad pixels, and reduces acquisition time (fewer image frames) for generating the desired Digital Elevation Map (DEM). We have shown 25X image resolution enhancement by processing 20 consecutive flash lidar frames recorded from moving trucks, dynamic testing at NASA LaRC gantry facility, Drone flight tests [6,7], and a helicopter flight test. The SR algorithm also provides the six-degree-of-freedom (6-DOF) relative state vector (position and attitude) of the host vehicle with higher precision than most inertial measurements.

Another advantage of flash lidar is the ability to perform other important functions that can help reliable precision landing at the designated location. As explained in section III, the flash lidar can measure vehicle altitude from very long distances and enable Terrain Relative Navigation [9]. Since flash lidar is essentially a 3-D video camera, it can also be used as a video navigation sensor enabling Hazard Relative Navigation after the selection of landing location.

II. Performance Characterization and Demonstration Tests

We built a breadboard unit with an integrated real-time SR algorithm for conducting a series of ground and airborne tests aimed at characterizing our lidar technique for HDA. This lidar used a linear-mode flash lidar camera, consisting of a focal plane array and associated control electronics, developed by Advanced Scientific Concepts (ASC). The lidar was set to acquire range image frames at 20 Hz for the application of the SR algorithm. The algorithm processed the image frames as they were received by the processer producing high resolution DEMs at 1 Hz rate with about 30 msec latency.

We conducted a set of characterization tests at the NASA LaRC's lidar test range and gantry facilities, followed by a drone flight test [10]. The gantry and drone flight tests allowed for pointing the lidar toward the ground and illuminating all pixels as opposed to horizontal tests pointing to targets of limited sizes that do not completely fill the lidar FOV. Fig. 1 shows the breadboard lidar on the drone flying over a clear area at NASA LaRC. For gantry and drone tests, several rectangular and hemispherical objects with different sizes, from 5 cm to 1 m, placed on the ground as calibrated targets (see Fig. 2). The reflectivity, shape, size, and the placement of these targets were selected so that the primary performance parameters, including resolution, range precision, and hazard detection threshold could be determined. The gantry and drone flight tests were conducted to their maximum operational limits of 65 m and 110 m height above the ground, respectively.

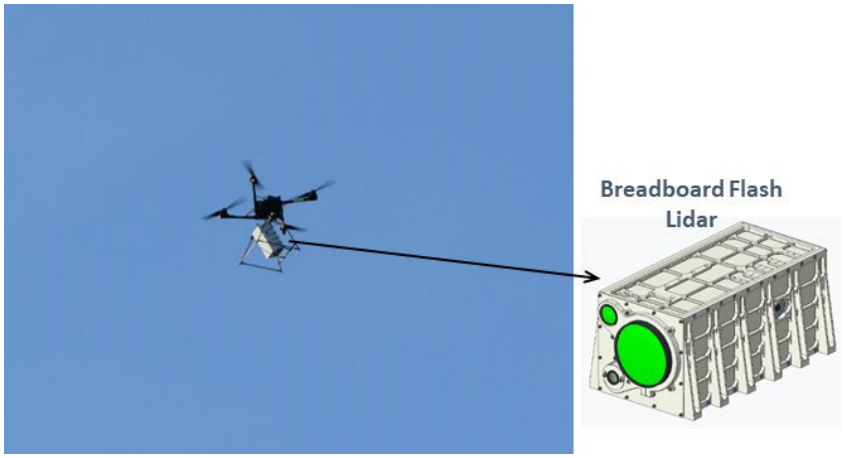

Fig. 1 Drone flight test of the breadboard lidar.

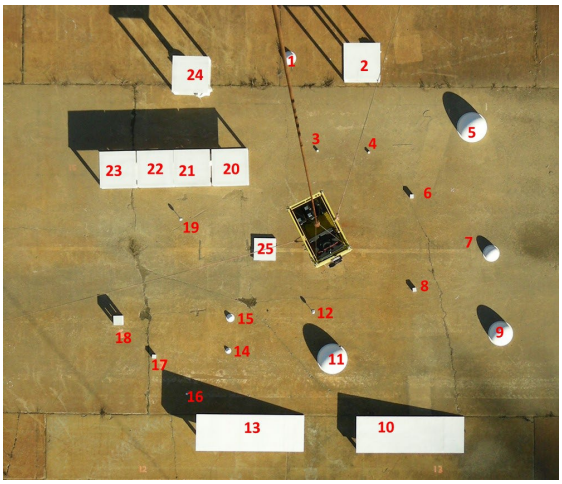

Fig. 2 Registered calibrated targets for gantry and drone flight tests.

After completion of the characterization tests, a helicopter flight test campaign was conducted in 2023 at the Blue Origin's Lunar Terrain Field in west Texas that was specifically built for testing landing sensors (see Fig. 3). This helicopter flight test allowed for simulating the lunar landing scenarios by flying along different slanted trajectories toward the Lunar Terrain Field (LTF).

Fig. 3 A view of the Blue Origin's Lunar Terrain Field with rock piles and craters.

An example of the helicopter flight test data is provided in Fig. 4 showing a single range image frame from about 200 m distance that are generated at 20 Hz and the DEM generated 1 Hz. As can be seen, some of smaller rock piles are not resolved in the 3-D range image but clearly detected in the DEM created by the SR algorithm.

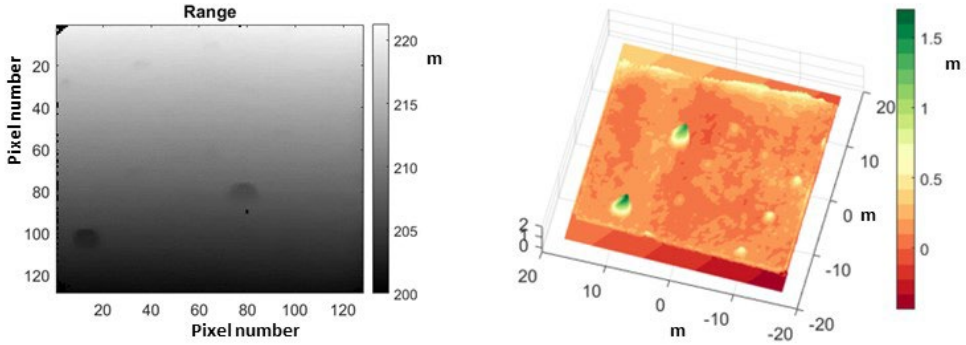

Fig. 4 A example of helicopter flight test results, showing a single range image (left) and a high resolution DEM generated in real-time at 1 Hz by applying SR algorithm to 20 consecutive range image frames (right).

Another example is provided in Fig. 5 where a lidar-generated DEM is provided (a) along with the corresponding area on a synthetic image of the LTF (b). This particular DEM is generated from 150 m slant range. Fig. 6 compares the lidar generated DEM with the truth DEM by plotting the elevation profiles along two lines drawn on the DEM and the LTF image in Fig. 5. These elevation profiles show very good agreement between the truth DEM and the lidar generated DEM. The difference in elevations is within a few centimeters, part of which is due to the fact that the truth DEM is not an exact representation of the LTF at the time of the flight test. The truth DEM was generated several years earlier, and the field had experienced significant changes due to weather and natural erosion.

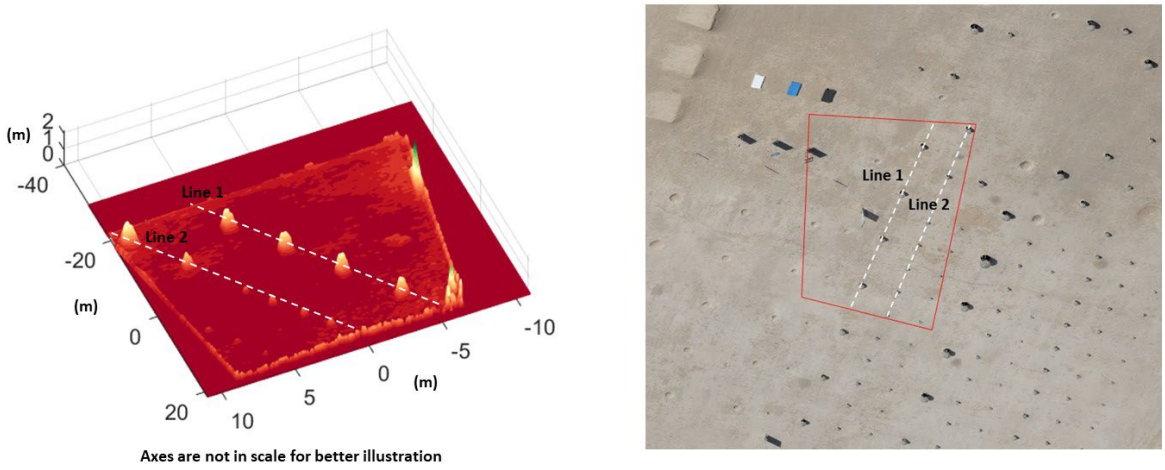

(a) **(b)**

Fig. 5 DEM of a section of the LTF (a) and the corresponding area on a synthetic image of the LTF (b).

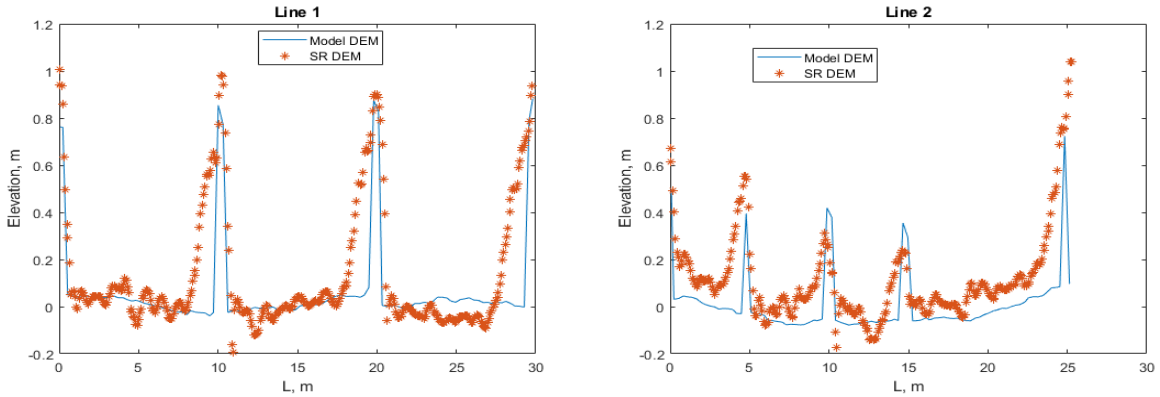

Fig. 6 Elevation profiles (red dots) along two lines on the DEM of Fig. 5 compared with the truth DEM (blue line).

The results of this flight test showed 100% hazard detection without any false alarms from 250 m altitude at different flight trajectory angles, from 30 to 65 degrees. Since the DEMs are generated at 1 Hz rate with insignificant latency, multiple DEMs were generated during each flight pass toward the ground. The results of this helicopter flight test demonstrated the viability of our lidar technique in detection of terrain hazards and selection of safe landing locations for future landing missions.

III. Terrain Sensing Lidar Prototype

The results of the dynamic tests described above were used for the design and build of a prototype system. The prototype unit includes several upgrades over the breadboard system such as higher transmitted pulse energy by approximately 5X, extended HDA operational range by 5X, and incorporation of multi-mode capability for performing long range altimetry, Terrain Relative Navigation (TRN), and Hazard Relative Navigation (HRN). The

prototype system, as shown in Fig. 7, has a compact design with a total mass of 6.5 kg which includes the real-time image processor and command/data interface with the host vehicle. The operational range of this lidar, in HDA mode with entire detector array illuminated, has been measured to be 1.3 km.

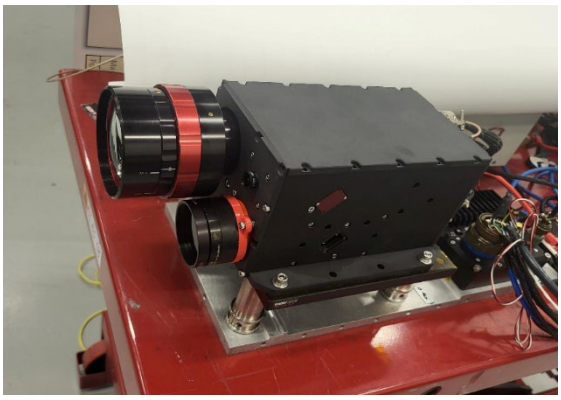

Fig. 7 Terrain Sensing Lidar (TSL) prototype with multi-functional capability.

A notional operational scenario of this lidar, we refer to Terrain Sensing Lidar (TSL), is shown in Fig. 8 in the context of a lunar landing. The TSL begins its operation after a deorbit maneuver at about 50 km above the ground. At this stage, the lidar transmitter beam is focused to illuminate only a few pixels, out of 16,384 pixels, in the center of the detector array to measure range to the ground. The lidar has an operational range of 1.3 km when all of the detector pixels are illuminated. Reducing the divergence of the lidar transmitter beam to a fraction of its receiver field of view increases its operational slant range to over 50 km from 1.3 km. The ground-relative altitude measurements provided by the TSL reduces the vehicle position error significantly since the Inertial Measurement Unit (IMU) suffers from drastic drift over the travel time from the Earth. The IMU drift error can be about 1 km for a Moon-bound vehicle and 10 km for Mars. Accurate altitude data reduces position error to a few hundred meters.

When the altitude drops to about 20 km, the lidar beam is expanded to illuminate a few hundred detector pixels. In this phase, the TSL generates relatively low-resolution elevation data of the terrain below which are subsequently compared with stored maps of known surface features such as craters. This process, referred to as TRN, further reduces the vehicle's relative position error from hundreds of meters to tens of meters.

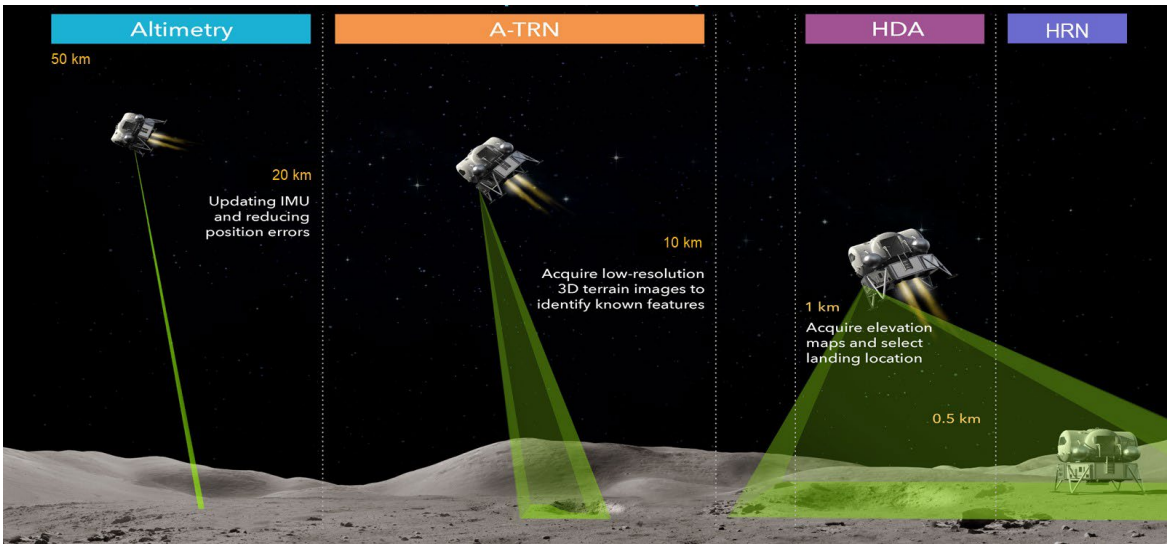

Fig. 8 An operational concept of multi-mode Terrain Sensing Lidar (TSL) for lunar landing.

From about 1 km to 0.5 km altitude, the flash lidar operates with its full field of view, generating a high-resolution elevation map of the landing area as described in previous section. This elevation map is then processed to identify hazardous features such as rocks, craters, and steep slopes, and to determine the most suitable landing

location (HDA function). Each generated DEM will cover approximately 100 m x 100 m area and can detect hazards greater than 30 cm in radius. As noted earlier, each DEM and the associated hazard maps can be generated in 1 second with a latency of the order of tens of milliseconds [11]. Therefore, multiple DEMs can be generated in this phase which can be several seconds in duration. These additional DEMs which can be either used for covering a larger area than the specified 100 m x 100 m or for further enhancing the resolution of the DEM and verification of the selected best landing location.

The TSL can continue acquiring range images after selection of the landing location and use the terrain features within the landing site for guiding the vehicle toward the landing location. This phase of the TSL operation is referred to as HRN. The TSL operation terminates at approximately 50 m above the ground before the vehicle thrusters create a dust plume. Table 1 summarizes the specifications of the TSL.

Table 1. TSL Specifications

Parameter	Operational Range
Altimetry Operational Range	50 km – 50 m
TRN Operational Range	20 km – 10 km
HDA Operational Slant Range	1.3 km – 0.7 km
HRN Operational Range	0.5 km – 50 m
DEM Update Rate	1 Hz
State Vector Update Rate	20 Hz
Mass	6.5 kg
Power	47 W

The TSL prototype is suitable for drone, helicopter, and fixed-wing aircraft flight tests and demonstration of its capabilities for landing on the Moon, Mars, and other destinations in our solar system. These flight tests will help to assess the TSL performance for each of the four functions as described above and serve as a stepping stone for the development of spaceflight units.

IV.Conclusion

A multi-functional lidar sensor based on linear-mode flash lidar technology and by utilizing a novel Super-Resolution algorithm has been developed for performing four key functions for precision and safe landing. This lidar sensor, referred to as Terrain Sensing Lidar, can enable long distance altimetry, Terrain Relative Navigation, Hazard Detection and Avoidance, and Hazard Relative Navigation thus meeting the needs of future landing missions requiring precision safe landing at designated locations on the Moon or other destinations in the solar system. Previously, a breadboard system was developed and subjected to a series of static and dynamic tests leading to a helicopter flight test campaign that successfully demonstrated its Hazard Detection and Avoidance capability. The results of these tests helped to design and build a multi-functional prototype system that can meet the requirements of most landing missions that are currently under consideration. The compact and robust design of this prototype sensor allows for flight tests onboard drones as well as helicopter and fixed-wing aircraft platforms that can pave the path for the development of spaceflight units and support the development of an optimum concepts of operation for each specific mission.

Acknowledgments

The authors are grateful to the Center Director's Office and the Space Technology and Exploration Directorate at NASA Langley Research Center for their continued support. The authors also acknowledge the Blue Origin team, in particular Tyler Rosenberger, Kyle Hickman, Michael Forrest, and Zhuoyuan Song, for facilitating the helicopter flight test campaign, supporting post flight data analysis, and for several years of collaboration on tests and analyses of hazard detection lidars.

References

[1] Epp, C. D., Robinson, E. A., and Brady, T., "Autonomous Landing and Hazard Avoidance Technology (ALHAT)", Proc. of IEEE Aerospace Conference, paper no. 1644, 2008.

[2] Carson III, J. M., Robertson, E. A., Trawny, N., and Amzajerdian, F., “Flight Testing ALHAT Precision Landing Technologies Integrated Onboard the Morpheus Rocket Vehicle," Proc. AIAA Space 2015 Conference & Exposition, Pasadena, CA, 2015.
[3] Farzin Amzajerdian, Vincent E. Roback, Alexander E. Bulyshev, Paul F. Brewster, William A. Carrion, Diego F. Pierrottet, Glenn D. Hines, Larry B. Petway, Bruce W. Barnes, and Anna M. Noe, “Imaging flash lidar for safe landing on solar system bodies and spacecraft rendezvous and docking,” Proc. SPIE Vol 9465, 2015.
[4] Farzin Amzajerdian, Vincent E. Roback, Alexander Bulyshev, Paul F. Brewster, Glenn D. Hines, “Imaging Flash Lidar for Autonomous Safe Landing and Spacecraft Proximity Operation,” AIAA SPACE Forum, (AIAA 2016-5591) 10.2514/6.2016-5591, 2016.
[5] Alexander Bulyshev and Farzin Amzajerdian, “Hazard Avoidance Algorithm for a 3-D Imaging Flash Lidar Utilizing Multi-Frame Super-Resolution Technique,” AIAA Guidance, Navigation, and Control Conference, AIAA SciTech Forum, 2023.
[6] Vincent E. Roback , Diego F. Pierrottet, Farzin Amzajerdian, Bruce W. Barnes, Glenn D. Hines, Larry B. Petway, Paul F. Brewster, Kevin S. Kempton, and Alexander E. Bulyshev, “Lidar sensor performance in closed-loop flight testing of the Morpheus rocket-propelled lander to a lunar-like hazard field,” Proc. of AIAA Science and Technology Forum and Exposition, 2015.
[7] A. Bulyshev, F. Amzajerdian, V. E. Roback, G. Hines, D. Pierrottet, and R. Reisse, “Three-dimensional super-resolution: theory, modeling, and field test results,” Appl. Opt. 53(12), 2583, 2014.
[8] Alexander Bulyshev, Farzin Amzajerdian, Eric Roback, Robert Reisse, “A super-resolution algorithm for enhancement of flash lidar data: flight test results,” Proc. SPIE Vol. 9020, 2014.
[9] Johnson, A.E., and Montgomery, J., “An Overview of Terrain Relative Navigation for Precise Lunar Landing,” IEEE Aerospace Conference, 2008.
[10] F. Amzajerdian, P. Brewster, B. Meadows, R. Haq,, A. Bulyshev, G. Shen, S. Bieniawski, B. P. Smith, and D. Kipp. “Performance of Flash Lidar with real-time image enhancement algorithm for Landing Hazard Avoidance,” AIAA SciTech, San Diego, 2022.
[11] Alexander Bulyshev and Farzin Amzajerdian, “Hazard Avoidance Algorithm for a 3-D Imaging Flash Lidar Utilizing Multi-Frame Super-Resolution Technique,” AIAA Guidance, Navigation, and Control Conference, AIAA SciTech Forum, 2023.